Hydroelastic linearized vibrations taking into account prestressed effects due to internal liquid weight: Numerical vs. experimental results

Christophe Hoareau, Jean-François Deü, Roger Ohayon

Hydroelastic linearized vibrations taking into account prestressed effects due to internal liquid weight: numerical vs. experimental results

C. Hoareau, J.-F. Deü, R. Ohayon

Laboratoire de Mécanique des Structures et des Systèmes Couplés (LMSSC)
Structural Mechanics and Coupled System Laboratory
Conservatoire national des arts et métiers (Cnam)

292 Rue Saint-Martin, 75003 Paris, France

Abstract

This paper concerns the numerical simulation of the hydroelastic vibrations of an elastic tank containing a free surface liquid, around a geometrically nonlinear equilibrium configuration that takes into account the prestress effect due to the liquid weight. The computational methodology is the following. Firstly, the hydrostatic pressure on the fluid-structure interface is considered as a non-uniform follower force which depends on the liquid height. Therefore, the prestressed equilibrium at a given free-surface level, called current configuration in the paper, is computed as a geometrically nonlinear problem, in which the height of the liquid is considered as an evolution parameter. We start from an empty structure, defined as the reference configuration, which is progressively filled to reach the level of the chosen configuration. Therefore the calculation of hydroelastic vibrations of a tank filled with liquid as a function of a emptying rate is straightforward. The methodology is validated with experimental results extracted from literature.

Keywords: Liquid weight, Pressure prestress effect, Geometrical nonlinearity, Hydroelastic vibrations, Finite element method

⋆Hydroelastic linearized vibrations taking into account prestressed effects due to internal liquid weight: numerical vs. experimental results

*Corresponding author
Email address: christophe.hoareau@lecnam.net (Laboratoire de Mécanique des Structures et des Systèmes Couplés (LMSSC)
Structural Mechanics and Coupled System Laboratory
Conservatoire national des arts et métiers (Cnam))
URL: http://www.lmssc.cnam.fr/ (Laboratoire de Mécanique des Structures et des Systèmes Couplés (LMSSC)
Structural Mechanics and Coupled System Laboratory
Conservatoire national des arts et métiers (Cnam))

1. Introduction

This study deals with a hydroelastic problem, namely the linearized vibrations of elastic structures, filled with an inviscid incompressible fluid, taking into account the prestress effect due to the fluid weight at the fluid-structure interface and neglecting the solid weight. Note that the weight effect in structural vibrations has already been the subject of several analyses (see e.g. [1]). Let us recall that linearized hydroelastic vibration analysis is of great interest in the study of liquid rocket launchers control and stability. Generally, in hydroelastic vibrations, the elasticity of the tank is of prime importance together with the kinetic energy of the liquid considered as incompressible (the called added mass effect [2, 3]). This means that compressibility effects of the liquid (its potential energy) as well as the effects of sloshing of the free surface (potential energy due to gravity and/or surface tension) can be neglected [4]. Of course, the gravity effects are present to define the equilibrium static configuration around which the vibrations are studied. Furthermore, those tanks can be pressurized, and effects of the pressure above the liquid can be significant especially for liquid propelled launchers. They have been taken into account through classical prestress geometrical terms considering specific linearization approaches [5, 6]. For general nonlinear fluid-structure interaction in the time domain, see for instance [7]. According to authors knowledge, the weight of the liquid on the structural vibrations has never been taken into account in coupled three-dimensional fluid-structure computations models [8]. This constitutes the first originality of the paper. Nevertheless, it should be mentioned that semi-analytical approaches exist for the study of pre-deformed membrane in a semi-infinite fluid medium [9] or for rigid cylindrical tank with an elastic bottom [10].

In addition, for liquid propelled launchers, the evolution of the frequencies as a function of the emptying rate is of prime importance. The period of vibration of the liquid structure system being very small compared to the time needed to emptying the tank during the launch, the vibrations of the system are classically performed for various liquid height which is considered as an evolution parameter. One major interest of the method presented here is to compute the vibrations considering nonlinear static prestressed state obtained through a procedure considering the weight of the liquid, depending on its height, from an empty situation up to a required filling level. It allows the computation of the hydroelastic vibrations corresponding to the appropriate liquid height. This constitutes the second originality of the approach.

Usually, the effects of geometric nonlinearities of prestressed type, due to the presence of the liquid (effects of gravity linked to the hydrostatic pressure which induces a non-uniform following force) are generally neglected in fluid-structure vibrations problems. Therefore, it is important to assess these effects on the linearized vibrations analysis around the prestressed state. Studies concerning the estimation of the prestress, from a nonlinear static evolution problem due internal or external pressure, can be found in [11, 12, 13] and notably for hydrostatic pressure in [14, 15, 16].

Throughout all the paper, in static as in dynamic, it should be noted that the equation in the structure

and on the fluid-structure interface are considered through an appropriate reciprocal mapping on a reference configuration, defined as the structure empty structure (*in vacuo*). This constitutes also an original aspect of the computational approach.

The computational methodology used in this work is based on the finite element method for both the structure and fluid domains (see e.g.[2]). For FSI problems with external fluid, other numerical approaches can advantageously be used, such as the immersed methods [17]. To the best authors knowledge, very few experiments exist in literature to quantify the prestressed effect investigated in this contribution. The computational results presented in this work can still be compared with the experimental results given in [18] in order to validate the numerical developments.

The outline of the paper is as follows. Following this introduction, in Section 2, the nonlinear static liquid-structure computation as function of the liquid height is introduced. In Section 3, the linearized harmonic hydroelastic problem is developed. In Section 4, the computational methodology is presented. In Section 5, comparison and validation with experiments are discussed. Finally, in Section 6 conclusion is given followed by references.

2. Nonlinear static liquid-structure computation as function of the liquid height

For general studies on theoretical and computational nonlinear structural mechanics, see references [19, 20, 21, 22, 23].

2.1. Definition of the parameterized prestressed configuration

The structure is supposed to be nonlinear elastic isotropic and relevant of Saint-Venant Kirchhoff constitutive relations (i.e. large displacements and small strain assumption). We define as the prestressed configuration, the stresses in the structure containing the liquid given in the called current configuration $\Omega'_{\rm s}$ such that $\partial\Omega_{\rm s} = \Sigma'_{\rm i} \cup \Sigma'_{\rm u} \cup \Sigma'_{\rm e}$ where $\Sigma'_{\rm i}$ is the fluid-structure interface, $\Sigma'_{\rm u}$ is the surface with prescribed displacements and $\Sigma'_{\rm e}$ is the surface of application of external load (see Fig. 1). Let $(\boldsymbol{e}_x, \boldsymbol{e}_y, \boldsymbol{e}_z)$ be the orthogonal unit vectors which define the Cartesian coordinates system. Concerning the liquid with horizontal free-surface under constant gravity force $\boldsymbol{g} = -g\boldsymbol{e}_{\rm z}$, the equations are relevant of the classical hydrostatic equation due to gravity. We do not consider here surface tension of the free surface. Thus, the prestressed state in the structure is only due to the weight of liquid seen as non-uniform follower forces [24, 25] as shown in Fig 1. The liquid pressure on the interface only depends on the wetted interface position for a given configuration.

In practice, this problem will be solved progressively by filling the tank from an empty state until the prestressed configuration. Thus, the problem is treated as a parameterized problem depending on the fluid height denoted by l.

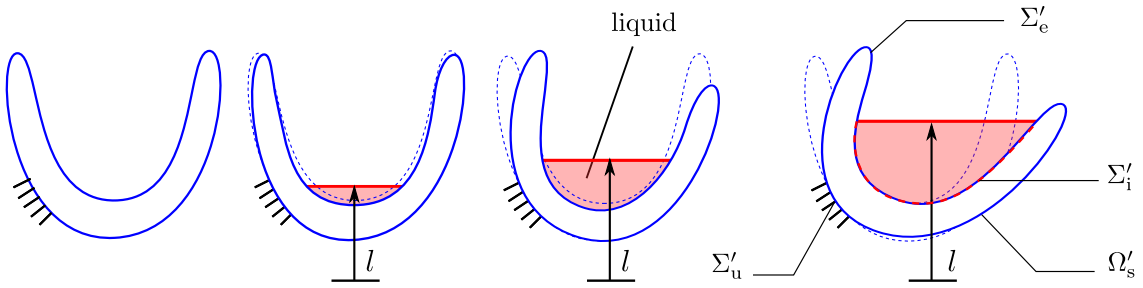

Figure 1: Various filling liquid levels in an elastic tank considering an evolution of the liquid height l.

2.2. Definition of the reference configuration

It is important to note (see [15]) that we will consider as the reference configuration, the empty structure, at equilibrium, at rest in a Galilean frame of reference. More precisely, this means that the current structural configuration, with the fluid structure interface, will be treated through an appropriate reciprocal mapping on this reference configuration as seen in Fig 2.

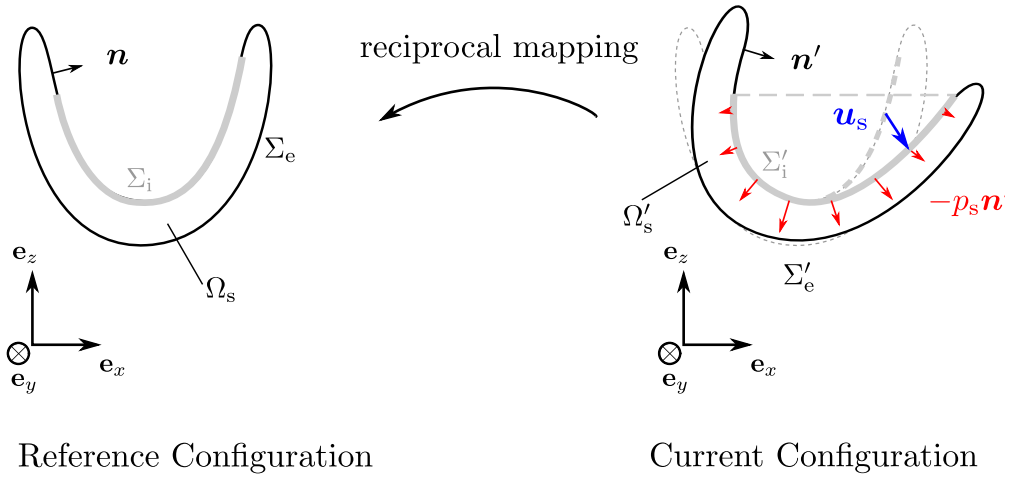

Figure 2: Reciprocal mapping of the liquid-structure interface from the current configuration on the reference configuration.

2.3. Computation of the prestressed state as a function of the liquid height

The structural displacement field is denoted by $\boldsymbol{u}_{\mathrm{s}} = u_{\mathrm{s}}\boldsymbol{e}_x + v_{\mathrm{s}}\boldsymbol{e}_y + w_{\mathrm{s}}\boldsymbol{e}_z$ in a Cartesian coordinate system. Thus, the current position $\boldsymbol{x}' = x'\boldsymbol{e}_x + y'\boldsymbol{e}_y + z'\boldsymbol{e}_z$ is defined by:

$$\boldsymbol{x}' = \boldsymbol{x} + \boldsymbol{u}_{\mathrm{s}} \tag{1}$$

where $\boldsymbol{x} = x\boldsymbol{e}_x + y\boldsymbol{e}_y + z\boldsymbol{e}_z$ is the reference position of a material point in the structure on its reference configuration Ω_{s} bounded by $\partial\Omega_{\mathrm{s}} = \Sigma_{\mathrm{i}} \cup \Sigma_{\mathrm{u}} \cup \Sigma_{\mathrm{e}}$, which are respectively, the interface, the surface with

prescribed displacement and the distributed load surfaces mapped on the reference configuration. It should be noted that the nonlinear static problem is expressed only in terms of structural displacement. The static pressure, which depends on the structural displacement, is defined on the current fluid-structure interface Σ_{i}', considered on a structural material point such that:

$$p_{\mathrm{s}}(l;\boldsymbol{u}_{\mathrm{s}}) = \begin{cases} 0 & \text{if} \quad z' \geq l \\ -\rho_{\mathrm{f}} g(z'-l) & \text{if} \quad z' < l \end{cases} \tag{2}$$

where $z' = (\boldsymbol{x}+\boldsymbol{u}_{\mathrm{s}})\cdot\boldsymbol{e}_{\mathrm{z}}$.

Let the transformation gradient and the Green-Lagrange strain operator, with respect to the reference position $\boldsymbol{x}$ be defined as:

$$\boldsymbol{F}(\boldsymbol{u}_{\mathrm{s}}) = \boldsymbol{I} + \mathbf{Grad}\boldsymbol{u}_{\mathrm{s}} \tag{3}$$

$$\boldsymbol{E}(\boldsymbol{u}_{\mathrm{s}}) = \frac{1}{2}(\boldsymbol{F}^{\mathrm{T}}(\boldsymbol{u}_{\mathrm{s}})\boldsymbol{F}(\boldsymbol{u}_{\mathrm{s}}) - \boldsymbol{I}) \tag{4}$$

The determinant of the transformation gradient is denoted by J as:

$$J(\boldsymbol{u}_{\mathrm{s}}) = \det(\boldsymbol{F}(\boldsymbol{u}_{\mathrm{s}})) \tag{5}$$

For sake of brevity, the structural body forces are neglected. The given force depends upon the liquid height l as seen in Eq. (2). We will consider here the structure as clamped on Σ_{u}. The structural mechanical equations are given on the reference configuration Ω_{s}, considering $\boldsymbol{F} = \boldsymbol{F}(\boldsymbol{u}_{\mathrm{s}})$, $\boldsymbol{E} = \boldsymbol{E}(\boldsymbol{u}_{\mathrm{s}})$ and $J = J(\boldsymbol{u}_{\mathrm{s}})$, such that:

$$-\mathbf{Div}(\boldsymbol{F}\boldsymbol{S}) = \boldsymbol{0} \qquad \text{in} \quad \Omega_{\mathrm{s}} \tag{6}$$

$$\mathcal{D} : \boldsymbol{E} = \boldsymbol{S} \qquad \text{in} \quad \Omega_{\mathrm{s}} \tag{7}$$

$$\boldsymbol{F}\mathbf{S}\boldsymbol{n} = J\boldsymbol{F}^{-\mathrm{T}} p_{\mathrm{s}}\boldsymbol{n} \qquad \text{on} \quad \Sigma_{\mathrm{i}} \tag{8}$$

$$\boldsymbol{u}_{\mathrm{s}} = \boldsymbol{0} \qquad \text{in} \quad \Sigma_{\mathrm{u}} \tag{9}$$

where Eq. (6) is the balance of linear momentum, Eq. (7) is the Saint-Venant Kirchhoff constitutive relation, which links the second Piola-Kirchhoff stress $\boldsymbol{S}$, consequently $\boldsymbol{S} = \boldsymbol{S}(\boldsymbol{u}_{\mathrm{s}})$, where $\mathcal{D}$ is a constant fourth order tensor of elasticity in which the notation ":" correspond to the trace operator, Eq. (8) is the equilibrium of follower forces surface traction and Eq. (9) correspond to a fixed displacement boundary condition. We recall that the pressure p_{s} depends of the unknown function $\boldsymbol{u}_{\mathrm{s}}$ and of the given data only (i.e. the height l). Let $\mathcal{C}_{\mathrm{u}}$ be the admissible space of regular displacement field:

$$\mathcal{C}_{\mathrm{u}} = \{\boldsymbol{v} \quad \text{"regular enougth"}, \quad \text{such that } \boldsymbol{v} = \boldsymbol{0} \quad \text{in} \quad \Sigma_{\mathrm{u}}\} \tag{10}$$

Let introduce a virtual displacement field $\delta\boldsymbol{u}$ in $\mathcal{C}_{\mathrm{u}}$. The static nonlinear problem consists in finding the displacement field $\boldsymbol{u}_{\mathrm{s}}$ in $\mathcal{C}_{\mathrm{u}}$ such that:

$$\delta W_{\mathrm{int}}(\boldsymbol{u}_{\mathrm{s}}, \delta\boldsymbol{u}) - \delta W_{\mathrm{ext}}(l;\boldsymbol{u}_{\mathrm{s}}, \delta\boldsymbol{u}) = 0, \qquad \forall\, \delta\boldsymbol{u} \ \in \mathcal{C}_{\mathrm{u}} \tag{11}$$

where $\delta W_{\rm int}$ and $\delta W_{\rm ext}$ are respectively the internal and external virtual works defined as:

$$\delta W_{\rm int}(\boldsymbol{u}_{\rm s}, \delta\boldsymbol{u}) = \int_{\Omega_{\rm s}} \delta\boldsymbol{E}(\boldsymbol{u}_{\rm s}, \delta\boldsymbol{u}) : \boldsymbol{S}(\boldsymbol{u}_{\rm s}) d\Omega \tag{12}$$

$$\delta W_{\rm ext}(\boldsymbol{u}_{\rm s}, \delta\boldsymbol{u}) = \int_{\Sigma_{\rm i}} -p_{\rm s}(l;\boldsymbol{u}_{\rm s})\, J(\boldsymbol{u}_{\rm s}) \boldsymbol{F}^{-{\rm T}}(\boldsymbol{u}_{\rm s}) \boldsymbol{n} \cdot \delta\boldsymbol{u}\, d\Sigma \tag{13}$$

where the term $\delta\boldsymbol{E}$ is the virtual Green-Lagrange matrix defined as follows:

$$\delta\boldsymbol{E}(\boldsymbol{u}_{\rm s}, \delta\boldsymbol{u}) = \frac{1}{2}\left(\delta\boldsymbol{F}^{\rm T}(\delta\boldsymbol{u})\boldsymbol{F}(\boldsymbol{u}_{\rm s}) + \boldsymbol{F}^{\rm T}(\boldsymbol{u}_{\rm s})\delta\boldsymbol{F}(\delta\boldsymbol{u})\right) \tag{14}$$

with

$$\delta\boldsymbol{F}(\delta\boldsymbol{u}) = \mathbf{Grad}\delta\boldsymbol{u} \tag{15}$$

The resolution of the problem Eq. (11) is based on the finite element approach. It should be noted that, for computational and software facilities, the computation of the static response of the structure, for each level of liquid, is carried out on the reference configuration defined in Section 2.2. A finite element discretization of the 3D domain $\Omega_{\rm s}^{\rm h}$ and its boundaries $\partial\Omega_{\rm s}^{\rm h} = \Sigma_{\rm i}^{\rm h} \cup \Sigma_{\rm u}^{\rm h} \cup \Sigma_{\rm e}^{\rm h}$ is now considered (see Fig. 1 for the continuous representation on the current configuration). The discretized displacement field and its virtual form are denoted $\boldsymbol{u}_{\rm s}^{\rm h}$ and $\delta\boldsymbol{u}^{\rm h}$ such that:

$$\boldsymbol{u}_{\rm s}^{\rm h} = \mathbf{N}_{\rm u}\mathbf{u}_{\rm s} \quad \text{and} \quad \delta\boldsymbol{u}^{\rm h} = \mathbf{N}_{\rm u}\delta\mathbf{u} \tag{16}$$

where $\mathbf{N}_{\rm u}$ is a known shape function matrix, $\mathbf{u}_{\rm s}$ is a unknown nodal vector and $\delta\mathbf{u}$ is the associated virtual nodal displacement. Considering Eq. (11), the discretized problem consists in finding $\mathbf{u}$ such that:

$$\mathbf{f}_{\rm int}(\mathbf{u}_{\rm s}) - \mathbf{f}_{\rm ext}(l;\mathbf{u}_{\rm s}) = \mathbf{0} \tag{17}$$

where $\mathbf{f}_{\rm int}$ and $\mathbf{f}_{\rm ext}$ are respectively the internal and external finite element forces defined as:

$$\delta W_{\rm int}(\boldsymbol{u}_{\rm s}^{\rm h}, \delta\boldsymbol{u}^{\rm h}) = \delta\mathbf{u}^{\rm T}\mathbf{f}_{\rm int}(\mathbf{u}_{\rm s}) \tag{18}$$

$$\delta W_{\rm ext}(\boldsymbol{u}_{\rm s}^{\rm h}, \delta\boldsymbol{u}^{\rm h}) = \delta\mathbf{u}^{\rm T}\mathbf{f}_{\rm ext}(\mathbf{u}_{\rm s}) \tag{19}$$

The resolution of this nonlinear problem can be done considering a Newton-Raphson type algorithm. The geometrical, the material and the follower forces tangent stiffness matrices, respectively denoted by $\mathbf{K}_{\rm g}$, $\mathbf{K}_{\rm m}$ and $\mathbf{K}_{\rm f}$ defined as:

$$\frac{\partial\mathbf{f}_{\rm int}}{\partial\mathbf{u}_{\rm s}} = \mathbf{K}_{\rm g} + \mathbf{K}_{\rm m} \quad \text{and} \quad \frac{\partial\mathbf{f}_{\rm ext}}{\partial\mathbf{u}_{\rm s}} = \mathbf{K}_{\rm f} \tag{20}$$

Those operators are needed in the Newton-Raphson loop to obtain a quadratic convergence rate of the nonlinear solution. We will see in the following that $\mathbf{K}_{\rm m}$ and $\mathbf{K}_{\rm g}$ are also useful to take into account the prestressed effect on the linearized hydroelastic vibrations of the fluid-structure system. If the structure is completely free (i.e. no prescribed displacement), the tangent stiffness matrices should be adapted (e.g. through a pseudo-inverse analysis) to the singularity involved with respect to the rigid body motions.

3. Linearized harmonic hydroelastic problem

3.1. Liquid-structure assumption of the linearized hydroelastic problem

Let assume linearized vibrations of the fluid-structure system around a known equilibrium state (defined as the prestressed state which depends on the fluid height). The circular frequency is denoted by ω. Regarding the liquid, it is assumed to be inviscid, homogeneous and incompressible. Thus, those small motions are irrotational. Of course, for large amplitude nonlinear vibrations, this irrotational assumption would be not relevant but this case is out of the scope of this article. Nevertheless for moderate nonlinear vibrations, not considered here, the hypotheses of irrotationality could be maintained. Consequently, the equations of the fluid can be expressed through a scalar field namely the pressure field or the displacement potential field. We suppose that during those linearized vibrations, the potential energy of the free-surface, due to gravity and to surface tension, are negligeable with respect to the kinetic energy of the fluid and to the potential and kinetic energies of the structure. The consequent is that, for the fluid dynamic equation, the free-surface condition is expressed as a zero pressure condition (or zero potential of displacement condition). Let us recall that the gravity effect, on the fluid structure interface, has been of course taken into account for the static equilibrium and in the parameterized evolution of the static prestressed computations.

3.2. Linearized equations in the structure

The structural part of the system is supposed to be excited by a harmonic distributed load denoted by $\boldsymbol{f}$. The response of the prestressed system is defined by knowing the dynamic structural displacement $\boldsymbol{u}$, knowing the static displacement $\boldsymbol{u}_{\mathrm{s}}$ which is the results of the previous static nonlinear problems. Thus, the total displacement denoted by $\boldsymbol{u}_{\mathrm{tot}}$ is defined as:

$$\boldsymbol{u}_{\mathrm{tot}} = \boldsymbol{u}_{\mathrm{s}} + \boldsymbol{u} \tag{21}$$

The structure perturbation $\boldsymbol{u}$ is supposed to be small compared to the characteristic length of the structure t_{s} (e.g. the tank thickness) such that:

$$\frac{||\ \boldsymbol{u}\ ||_{\mathcal{L}_2}}{t_{\mathrm{s}}} << 1 \tag{22}$$

The current harmonic configuration is thus supposed to be the same configuration of the prestressed one (i.e. called the current configuration from the static problem). We take a Taylor series expansion of the virtual works, in which we retain up to the first order term in $\boldsymbol{u}$ written as follows:

$$\delta W_{\mathrm{acc}}(\boldsymbol{u}_{\mathrm{tot}}, \delta\boldsymbol{u}) = 0 \qquad - \quad \omega^2 m(\boldsymbol{u}, \delta\boldsymbol{u}) \tag{23}$$

$$\delta W_{\mathrm{int}}(\boldsymbol{u}_{\mathrm{tot}}, \delta\boldsymbol{u}) = \delta W_{\mathrm{int}}(\boldsymbol{u}_{\mathrm{s}}, \delta\boldsymbol{u}) \qquad + \quad k_{\mathrm{t}}(\boldsymbol{u}_{\mathrm{s}}; \boldsymbol{u}, \delta\boldsymbol{u}) \tag{24}$$

$$\delta W_{\mathrm{ext}}(h; \boldsymbol{u}_{\mathrm{tot}}, \delta\boldsymbol{u}) = \underbrace{\delta W_{\mathrm{ext}}(l; \boldsymbol{u}_{\mathrm{s}}, \delta\boldsymbol{u})}_{\text{static}} \qquad - \quad \underbrace{c(\boldsymbol{u}_{\mathrm{s}}; p, \delta\boldsymbol{u}) + f(\delta\boldsymbol{u})}_{\text{dynamic}} \tag{25}$$

where the term p corresponds to the dynamic pressure perturbations of the fluid at the fluid-structure interface such that:

$$p_{\mathrm{tot}} = p_{\mathrm{s}} + p \tag{26}$$

The terms involved in the linearized virtual acceleration and external works can be expressed on the reference configuration knowing the static displacement as follows:

$$m(\boldsymbol{u}, \delta\boldsymbol{u}) = \int_{\Omega_\mathrm{s}} \rho_\mathrm{s} \boldsymbol{u} \cdot \delta\boldsymbol{u} \, d\Omega \tag{27}$$

$$f(\delta\boldsymbol{u}) = \int_{\Sigma_\mathrm{e}} \boldsymbol{f} \cdot \delta\boldsymbol{u} \, d\Sigma \tag{28}$$

$$c(\boldsymbol{u}_\mathrm{s}; p, \delta\boldsymbol{u}) = \int_{\Sigma_\mathrm{i}} pJ(\boldsymbol{u}_\mathrm{s}) \boldsymbol{F}^{-\mathrm{T}}(\boldsymbol{u}_\mathrm{s}) \boldsymbol{n} \cdot \delta\boldsymbol{u} \, d\Sigma \tag{29}$$

where m is the virtual work induced by the inertia of the structure, f is the external fluctuation load and c is the coupling operator between the fluctuation of pressure and the virtual displacement. The virtual potential work from the tangent stiffness is defined as the sum of the geometrical and the material stiffness contributions. Then, the expression of the geometrical and material virtual stiffness works k_m and k_g are given as:

$$k_\mathrm{m}(\boldsymbol{u}_\mathrm{s}; \boldsymbol{u}, \delta\boldsymbol{u}) = \int_{\Omega_\mathrm{s}} \delta\boldsymbol{E}(\boldsymbol{u}_\mathrm{s}, \delta\boldsymbol{u}) : \mathcal{D} : [\boldsymbol{\varepsilon}(\boldsymbol{u}) + \boldsymbol{\gamma}(\boldsymbol{u}_\mathrm{s}, \boldsymbol{u})] \, d\Omega \tag{30}$$

$$k_\mathrm{g}(\boldsymbol{u}_\mathrm{s}; \boldsymbol{u}, \delta\boldsymbol{u}) = \int_{\Omega_\mathrm{s}} \boldsymbol{\gamma}(\boldsymbol{u}, \delta\boldsymbol{u}) : \mathcal{D} : \boldsymbol{S}(\boldsymbol{u}_\mathrm{s}) \, d\Omega \tag{31}$$

$$k_\mathrm{t} = k_\mathrm{m} + k_\mathrm{g} \tag{32}$$

where the operators $\boldsymbol{\varepsilon}$ and $\boldsymbol{\gamma}$, such that $\boldsymbol{\gamma}(\boldsymbol{u}, \boldsymbol{v}) = \boldsymbol{\gamma}(\boldsymbol{v}, \boldsymbol{u})$, depend on the gradient defined for given displacement fields $\boldsymbol{u}$ and $\boldsymbol{v}$ as follows:

$$\boldsymbol{\varepsilon}(\boldsymbol{u}) = \frac{1}{2}[\mathbf{Grad}^\mathrm{T} \boldsymbol{u} + \mathbf{Grad}\, \boldsymbol{u}] \tag{33}$$

$$\boldsymbol{\gamma}(\boldsymbol{u}, \boldsymbol{v}) = \frac{1}{2}[\mathbf{Grad}^\mathrm{T} \boldsymbol{u} \mathbf{Grad}\, \boldsymbol{v} + \mathbf{Grad}^\mathrm{T} \boldsymbol{v}\, \mathbf{Grad}\, \boldsymbol{u}] \tag{34}$$

Finally, the linearized harmonic problem consists in finding $\boldsymbol{u}_\mathrm{d} \in \mathcal{C}_\mathrm{u}$, knowing $\boldsymbol{u}_\mathrm{s}$ such that:

$$k_\mathrm{t}(\boldsymbol{u}_\mathrm{s}; \boldsymbol{u}, \delta\boldsymbol{u}) - c(\boldsymbol{u}_\mathrm{s}; p, \delta\boldsymbol{u}) - \omega^2 m(\boldsymbol{u}, \delta\boldsymbol{u}) = f(\delta\boldsymbol{u}), \ \forall\, \delta\boldsymbol{u} \ \in \ \mathcal{C}_\mathrm{u} \tag{35}$$

It can be seen that the operators k_m and k_g are symmetric in $\boldsymbol{u}$ and $\delta\boldsymbol{u}$. For the same reasons indicated in the previous section, the variational formulation of the local equations of the structure is posed on the reference configuration (see Section 2.2). That is why the coupled term representing the virtual work done by the dynamic pressure fluctuation p on the virtual normal displacement is written here not on the current configuration e.g. the structure filled with a liquid with free surface at height l, but on the reference configuration.

3.3. Linearized liquid equations

We are interested in the linearized vibrations of the liquid part. Since the liquid is irrotational, the displacement $\boldsymbol{u}_\mathrm{f}$ is derived from a potential displacement φ with respect to the liquid configuration at rest Ω'_f (the static liquid configuration) as:

$$\boldsymbol{u}_\mathrm{f} = \mathbf{grad}\varphi \tag{36}$$

The relations in the fluid domain involving the fluctuation of dynamic pressure p and the fluid motion such that are given as:

$$\operatorname{div} \boldsymbol{u}_{\mathrm{f}} = 0 \qquad \text{in} \quad \Omega'_{\mathrm{f}} \tag{37}$$

$$\mathbf{grad} p - \omega^2 \rho_{\mathrm{f}} \boldsymbol{u}_{\mathrm{f}} = \mathbf{0} \qquad \text{in} \quad \Omega'_{\mathrm{f}} \tag{38}$$

$$\boldsymbol{u}_{\mathrm{f}} \cdot \boldsymbol{n}' = \boldsymbol{u} \cdot \boldsymbol{n}' \qquad \text{in} \quad \Sigma'_{\mathrm{f}} \tag{39}$$

where the Eq. (37) is due to the incompressibility condition of the fluid motion, Eq. (38) correspond to the linear Euler equations and Eq. (39) corresponds to the normal displacement continuity between the normal fluid displacement field $\boldsymbol{u}_{\mathrm{f}} \cdot \boldsymbol{n}'$ and the normal solid displacement field $\boldsymbol{u} \cdot \boldsymbol{n}'$ on the liquid-structure interface denoted by $\boldsymbol{\Sigma}'_i$, in which $\boldsymbol{n}'$ denotes the external unit normal with respect to the solid. Considering the previous equations and the boundary conditions, expressed in term of potential displacement field φ as follows:

$$\begin{cases} \Delta\varphi = 0 & \text{in} \quad \Omega'_{\mathrm{f}} \qquad (40a) \\ \mathbf{grad}\varphi \cdot \boldsymbol{n}' = \boldsymbol{u} \cdot \boldsymbol{n}' & \text{in} \quad \Sigma'_{\mathrm{i}} \qquad (40b) \\ \varphi = 0 & \text{in} \quad \Gamma' \qquad (40c) \end{cases}$$

Eq. (40) involves only the geometry and shows that φ is a linear function of $\boldsymbol{u}_{\mathrm{f}}$ and that consequently, "the kinetic energy" of the incompressible liquid:

$$E_{\mathrm{kin}} = \frac{1}{2} \int_{\Omega'_{\mathrm{f}}} \rho_{\mathrm{f}} \mid \boldsymbol{\nabla}\varphi \mid^2 d\Omega \quad \left(\text{e.g.} \quad \frac{1}{2} \int_{\Omega'_{\mathrm{f}}} \rho_{\mathrm{f}} \mid \boldsymbol{u}_{\mathrm{f}} \mid^2 d\Omega \right), \tag{41}$$

is a quadratic form of $\boldsymbol{u}_{\mathrm{f}}$ such that the discretized form is the classical added mass matrix operator [2, 3]. Let us take the variational formulation of Eqs. (40) in the current configuration of the fluid:

$$\int_{\Omega'_{\mathrm{f}}} \mathbf{grad}\varphi \cdot \mathbf{grad}\delta\varphi \, d\Omega' + \int_{\Sigma'_{\mathrm{i}}} \boldsymbol{u} \cdot \boldsymbol{n}' \, \delta\varphi \, d\Sigma' = 0 \quad \forall \delta\varphi \in \mathcal{C}_\varphi \tag{42}$$

where $\mathcal{C}_\varphi$ the space of regular functions define on Ω'_{f} verifying Eq. (40c). It should be noted that the term expressed in Σ'_{i}, will be written, through the reciprocal mapping, on the reference configuration, defined in Section 2.2, such that:

$$\int_{\Sigma'_{\mathrm{i}}} \delta\varphi \boldsymbol{n}' \cdot \boldsymbol{u} \, d\Sigma' = \int_{\Sigma_{\mathrm{i}}} \delta\varphi \, J(\boldsymbol{u}_{\mathrm{s}}) \boldsymbol{F}^{-\mathrm{T}}(\boldsymbol{u}_{\mathrm{s}}) \boldsymbol{n} \cdot \boldsymbol{u} \, d\Sigma \tag{43}$$

For sake of brevity, we will use the same notations for the unknown fields $\boldsymbol{u}$ and φ defined either on Ω'_{f} and Σ'_{i} or Ω_{f} and Σ_{i}. Finally, the problem expressed in term of the variable φ (instead of p) and $\boldsymbol{u}$, can be written as follows:

$$h(\delta\varphi, \varphi) + c(\boldsymbol{u}_{\mathrm{s}}; \delta\varphi, \boldsymbol{u}) = 0, \qquad \forall \delta\varphi \in \mathcal{C}_\varphi \tag{44}$$

where the operator h correspond to the virtual work of the fluid kinetic energy and c corresponds to the liquid -structure coupling operator:

$$h(\varphi, \delta\varphi) = \int_{\Omega'_{\mathrm{f}}} \mathbf{grad}\varphi \cdot \mathbf{grad}\delta\varphi \, d\Omega' \tag{45}$$

$$c(\boldsymbol{u}_{\mathrm{s}}; \delta\varphi, \boldsymbol{u}) = \int_{\Sigma_i} \delta\varphi J(\boldsymbol{u}_{\mathrm{s}}) \boldsymbol{F}^{-\mathrm{T}}(\boldsymbol{u}_{\mathrm{s}}) \boldsymbol{n} \cdot \boldsymbol{u} \, d\Sigma \tag{46}$$

It should be noted that the discretization of the two terms of the variational formulation will be carried through two different aspects. The first contribution which involves only the displacement potential of the liquid will be done on this prestressed static configuration, around which we study the dynamic fluctuation. The second contribution, i.e. the coupled term, will be discretized on the reference configuration through a reciprocal mapping method. This is not an issue due to the fact that the construction of the operator is based on the known static displacement at the interface. The prestressed static configuration of the fluid can be done: (i) through a computation of a pre-deformed fluid mesh or (ii) considering a re-meshing of the fluid domain. The coupling term here gives a relation between the structural acceleration at the interface and the virtual potential of displacement.

3.4. Finite element discretization of the coupled problem

The potential of fluid displacement and the fluctuation of pressure are linked considering Eq. (36) and Eq. (38) such that:

$$p = \omega^2 \rho_{\mathrm{f}} \varphi \tag{47}$$

Consequently, the linearized structural virtual equation is written as:

$$k_{\mathrm{t}}(\boldsymbol{u}_{\mathrm{s}}; \boldsymbol{u}, \delta\boldsymbol{u}) - \omega^2 \rho_{\mathrm{f}} c(\boldsymbol{u}_{\mathrm{s}}; \varphi, \delta\boldsymbol{u}) - \omega^2 m(\boldsymbol{u}, \delta\boldsymbol{u}) = f(\delta\boldsymbol{u}), \qquad \forall\, \delta\boldsymbol{u} \in \mathcal{C}_{\mathrm{u}} \tag{48}$$

As done in Section 2, let introduce the finite element discretization of the fields $\boldsymbol{u}^{\mathrm{h}}$ and φ^{h} and their respective virtual fields. The discretized structural equation of Eq. (48) is given as:

$$\mathbf{K}_{\mathrm{t}}\mathbf{u} - \omega^2 \mathbf{M}\mathbf{u} - \omega^2 \rho_{\mathrm{f}} \mathbf{C}\boldsymbol{\varphi} = \mathbf{f} \tag{49}$$

Concerning the discretization of Eq. (44), the volumic term $h(\varphi, \delta\varphi)$ is discretized using the finite element discretization of $\Omega_{\mathrm{f}}^{\mathrm{h}}$. On the other hand, the second term of Eq. (44) which is the liquid-structure coupling term is discretized on the reference configuration (let us recall that the chosen configuration has been previously defined in Fig. 2 with no prestressed effect) using Eq. (46) :

$$\mathbf{H}\boldsymbol{\varphi} + \mathbf{C}^{\mathrm{T}}\mathbf{u} = \mathbf{0} \tag{50}$$

All the discretized operator are given as follows:

$$k_{\mathrm{t}}(\boldsymbol{u}_{\mathrm{s}}^{\mathrm{h}};\delta\boldsymbol{u}^{\mathrm{h}},\boldsymbol{u}^{\mathrm{h}}) \Rightarrow \delta\mathbf{u}^{\mathrm{T}}\mathbf{K}_{\mathrm{t}}(\mathbf{u}_{\mathrm{s}})\mathbf{u} \tag{51}$$

$$m(\delta\boldsymbol{u}^{\mathrm{h}},\boldsymbol{u}^{\mathrm{h}}) \Rightarrow \delta\mathbf{u}^{\mathrm{T}}\mathbf{M}\mathbf{u} \tag{52}$$

$$c(\boldsymbol{u}_{\mathrm{s}}^{\mathrm{h}};\delta\boldsymbol{u}^{\mathrm{h}},\varphi^{\mathrm{h}}) \Rightarrow \delta\mathbf{u}^{\mathrm{T}}\mathbf{C}(\mathbf{u}_{\mathrm{s}})\mathbf{u} \tag{53}$$

$$f(\delta\boldsymbol{u}^{\mathrm{h}}) \Rightarrow \delta\mathbf{u}^{\mathrm{T}}\mathbf{f} \tag{54}$$

$$h(\delta\varphi^{\mathrm{h}},\varphi^{\mathrm{h}}) \Rightarrow \delta\boldsymbol{\varphi}^{\mathrm{T}}\mathbf{H}\boldsymbol{\varphi} \tag{55}$$

$$c(\boldsymbol{u}_{\mathrm{s}}^{\mathrm{h}};\delta\varphi^{\mathrm{h}},\boldsymbol{u}^{\mathrm{h}}) \Rightarrow \delta\boldsymbol{\varphi}^{\mathrm{T}}\mathbf{C}(\mathbf{u}_{\mathrm{s}})\mathbf{u} \tag{56}$$

Taking into account the free-surface prescribed mandatory equation (40c), and for sake of simplification, using the same notations for $\mathbf{C}$ and $\mathbf{H}$, the coupled matrix system, resulting from Eq. (49) and Eq. (50) writes:

$$\left(\begin{bmatrix}\mathbf{K}_{\mathrm{t}} & \mathbf{O}\\ \mathbf{O} & \mathbf{O}\end{bmatrix} - \omega^2\begin{bmatrix}\mathbf{M} & \rho_{\mathrm{f}}\mathbf{C}\\ \rho_{\mathrm{f}}\mathbf{C}^{\mathrm{T}} & -\rho_{\mathrm{f}}\mathbf{H}\end{bmatrix}\right)\begin{pmatrix}\mathbf{u}\\ \boldsymbol{\varphi}\end{pmatrix} = \begin{pmatrix}\mathbf{f}\\ \mathbf{0}\end{pmatrix} \tag{57}$$

or equivalently

$$\mathbf{K}_{\mathrm{t}}\mathbf{u} - \omega^2(\mathbf{M} + \rho_{\mathrm{f}}\mathbf{M}_{\mathrm{a}})\mathbf{u} = \mathbf{f} \quad \text{with} \quad \mathbf{M}_{\mathrm{a}} = \mathbf{C}\mathbf{H}^{-1}\mathbf{C}^{\mathrm{T}} \tag{58}$$

Solving Eq. (58), we deduced directly $\boldsymbol{\varphi}$ and the discretized pressure $\mathbf{p}$ as follows:

$$\boldsymbol{\varphi} = -\mathbf{H}^{-1}\mathbf{C}^{\mathrm{T}}\mathbf{u} \quad \text{and} \quad \mathbf{p} = \omega^2\rho_{\mathrm{f}}\boldsymbol{\varphi} \tag{59}$$

in which $\mathbf{K}_{\mathrm{t}}$ is symmetric and $\mathbf{H}$, initially of kernel of dimension 1, is invertible using Eq. (40c), therefore the added mass matrix $\mathbf{M}_{\mathrm{a}}$ is a full, symmetric positive definite matrix, involving only structural fluid-structure interface degrees of freedom. In a practical situation, the matrix $\mathbf{H}^{-1}$ is never computed directly.

4. Computation methodology

The aim is to compute the linearized hydroelastic vibrations of an elastic tank prestressed by a liquid weight for various given liquid free-surface height $l_i \in [l_{\min}, l_{\max}]$. At first, for each values l_i, static nonlinear solutions $\mathbf{u}_{\mathrm{s}}^{(i)} = \mathbf{u}_{\mathrm{s}}(l_i)$ and the associated tangent stiffness matrix $\mathbf{K}_{\mathrm{t}}^{(i)} = \mathbf{K}_{\mathrm{t}}(l_i)$ are then computed step by step from $l_{\min}$ to $l_{\max}$ (see Section 2), which is an originality of the approach. We recall here that the discretized matrices are computed on the previously defined reference configuration in Section 2.2. Those tangent stiffness operators $\mathbf{K}_{\mathrm{t}}^{(i)}$ are stored and will be used for the calculation of the prestressed hydroelastic vibrations for various levels of liquid presented in Eq. (58). As mentioned in the previous section, the added mass matrix $\mathbf{M}_{\mathrm{a}}$ will never be constructed directly. Eq. (58) shows that the coupled eigenvalue hydroelastic problem is expressed only in terms of structural field unknown $\mathbf{u}$ (the potential of displacement and the pressure are then calculated on a straightforward manner by Eq. (59)), for a given level. The solution of Eq.

(58) can be searched using an appropriate basis of the structural admissible structural space $\mathcal{C}_{\rm u}$. Therefore, we can choose as a possible basis of $\mathcal{C}_{\rm u}$ the eigenvectors of the prestressed structure without taking into account liquid inertia:

$$[\mathbf{K}_{\rm t}^{(i)} - \omega^2 \mathbf{M}]\mathbf{u} = \mathbf{0} \tag{60}$$

The first N eigenvectors denoted by $\mathbf{u}_\alpha^{(i)} = \mathbf{u}_\alpha(l_i)$, normalized by the mass (i.e. $\mathbf{u}_\alpha^{(i)\rm T}\mathbf{M}\mathbf{u}_\alpha^{(i)} = 1$), and associated with the eigenvalues denoted by $\omega_\alpha^{2(i)}$, generate a basis denoted by $\mathcal{B}_u^{(i)}$ defined as:

$$\mathcal{B}_u^{(i)} = \left\{\mathbf{u}_\alpha^{(i)}\right\}_{\alpha=1\ldots m} \tag{61}$$

A remark has to be addressed at this point concerning the positivity of the tangent stiffness operator. For the practical application, we suppose that the action of the liquid weight in the structure tends to stiffen the system. Thus, we do not consider here the dynamic buckling, which can be the case for immersed structures. In the following, the vector of the basis $\mathcal{B}_u^{(i)}$ will called the prestressed dry modes. Of course question of truncation and related validations will be addressed later in the numerical application. Let us stress here that the computation of the added mass matrix no longer necessitates the direct inverse of a matrix. We proceed by considering known matrices $\mathbf{H}^{(i)} = \mathbf{H}(l_i)$ and $\mathbf{C}^{(i)} = \mathbf{C}(l_i)$ associated with the various liquid height. For each dry modes $\mathbf{u}_\alpha^{(i)}$, the computation of the liquid response in terms of displacement potential field can be obtained by solving the linear system of equation:

$$\mathbf{H}^{(i)}\boldsymbol{\varphi}_\alpha^{(i)} = -\mathbf{C}^{(i)\rm T}\mathbf{u}_\alpha^{(i)} \tag{62}$$

An approximation of $\mathbf{u}(l_i) = \mathbf{u}^{(i)}$ denoted by $\mathbf{u}_{\rm approx}^{(i)}$ is constructed as a linear combination of the truncated basis $\mathbf{u}_\alpha^{(i)}$:

$$\mathbf{u}_{\rm approx}^{(i)} \simeq \sum_{\alpha=1}^{m} q_\alpha^{(i)}\mathbf{u}_\alpha^{(i)} = \mathbf{B}_{\rm u}^{(i)}\mathbf{q}^{(i)} \quad \text{with} \quad \mathbf{B}_{\rm u}^{(i)} = \begin{bmatrix} \vdots & & \vdots \\ \mathbf{u}_1^{(i)} & \ldots & \mathbf{u}_m^{(i)} \\ \vdots & & \vdots \end{bmatrix} \quad \text{and} \quad \mathbf{q} = \begin{bmatrix} q_1^{(i)} \\ \vdots \\ q_m^{(i)} \end{bmatrix} \tag{63}$$

Then, we consider an approximation of the displacement potential $\boldsymbol{\varphi}(l_i) = \boldsymbol{\varphi}^{(i)}$ denoted by $\boldsymbol{\varphi}_{\rm approx}^{(i)}$ as a linear combination of the computed $\boldsymbol{\varphi}_\alpha(l_i) = \boldsymbol{\varphi}_\alpha^{(i)}$ as:

$$\boldsymbol{\varphi}_{\rm approx}^{(i)} = \sum_{\alpha}^{m} q_\alpha^{(i)}\boldsymbol{\varphi}_\alpha^{(i)} = \mathbf{B}_\varphi^{(i)}\mathbf{q}^{(i)} \quad \text{with} \quad \mathbf{B}_\varphi^{(i)} = \begin{bmatrix} \vdots & & \vdots \\ \boldsymbol{\varphi}_1^{(i)} & \ldots & \boldsymbol{\varphi}_m^{(i)} \\ \vdots & & \vdots \end{bmatrix} \tag{64}$$

Considering the left hand side of Eq. (49), and a left multiplication by $\mathbf{B}_{\rm u}^{(i)\rm T}$, the reduced hydroelastic problem projected of the prestressed dry modes is written as:

$$\underbrace{\mathbf{B}_{\rm u}^{(i)\rm T}\mathbf{K}_{\rm t}^{(i)}\mathbf{B}_{\rm u}^{(i)}}_{\mathbf{K}_{\rm r}^{(i)}}\mathbf{q}^{(i)} - \rho_{\rm f}\omega^2\underbrace{\mathbf{B}_{\rm u}^{(i)\rm T}\mathbf{C}^{(i)}\mathbf{B}_\varphi^{(i)}}_{\mathbf{M}_{\rm ar}^{(i)}}\mathbf{q}^{(i)} - \omega^2\underbrace{\mathbf{B}_{\rm u}^{(i)\rm T}\mathbf{M}^{(i)}\mathbf{B}_{\rm u}^{(i)}}_{\mathbf{M}_{\rm r}=\mathbf{I}}\mathbf{q}^{(i)} = \mathbf{0} \tag{65}$$

where the matrices $\mathbf{K}_{\rm r}^{(i)}$ and $\mathbf{M}_{\rm ar}^{(i)}$ are respectively the reduced tangent stiffness and added mass matrices which are $(N \times N)$ matrices defined as:

$$\mathbf{K}_{\rm r}^{(i)} = \begin{bmatrix} \ddots & & \\ & \omega_\alpha^{2(i)} & \\ & & \ddots \end{bmatrix} \quad \text{and} \quad \mathbf{M}_{\rm ar}^{(i)} = \begin{bmatrix} & \vdots & \\ \dots & m_{\alpha\beta}^{(i)} & \dots \\ & \vdots & \end{bmatrix} \tag{66}$$

where the reduced stiffness and mass matrices are diagonal matrices and the terms of the reduced added mass matrix are defined as:

$$m_{\alpha\beta}^{(i)} = \mathbf{u}_\alpha^{{\rm T}(i)} \mathbf{C}^{(i)} \boldsymbol{\varphi}_\beta^{(i)} = -\mathbf{u}_\alpha^{{\rm T}(i)} \mathbf{C}^{(i)} \mathbf{H}^{-1(i)} \mathbf{C}^{{\rm T}(i)} \mathbf{u}_\beta^{(i)} \tag{67}$$

Of course, the resulting reduced added mass matrix is symmetric positive definite.

The eigenvalue analysis of the reduced hydroelastic problem writes:

$$[\mathbf{K}_{\rm r}^{(i)} - \omega^2 (\mathbf{M}_{\rm ar}^{(i)} + \mathbf{I})]\mathbf{q} = \mathbf{0} \tag{68}$$

and gives the hydroelastic eigenmodes of the liquid structure problem.

5. Comparison and validation with experiments

5.1. Hydroelastic vibrations of a clamped circular plexiglass plate under a column of water

The computation methodology is applied to experiments carried out by M. Chiba [10]. It consists in evaluating the linearized hydroelastic vibrations of a thin circulate plate made of plexiglass under a column of water. The great interest of this example is that it highlights the prestressed effects due to the liquid weight on the linearized hydroelastic vibrations. The procedure is illustrated in Fig. 3. It consists in (i) computing the nonlinear static solutions of the elastic structure subjected to the hydrostatic pressure forces and (ii) establishing the linearized vibrations of the coupled system. The liquid is in contact with the structure upon the upper surface of the clamped plate, while the lower surface is free of charge. The liquid height is varying from $l_{\rm min} = 0$ mm to $l_{\rm max} = 250$ mm. The solid material parameters needed for the Saint-Venant Kirchhoff constitutive relations are the Young modulus $E = 6.9 \times 10^9$ Pa, the Poisson ratio $\nu = 0.38$ and the solid mass density $\rho_{\rm s} = 1.4 \times 10^3$ kg.m^{-3}. The liquid mass density is $\rho_{\rm f} = 1.0 \times 10^3$ kg.m^{-3}.

5.2. Preliminary nonlinear static evolution solution

The Fig. 4 illustrates the mesh parameterization of the elastic plate to compute the nonlinear static problem. The computation has been done with quadratic hexahedron elements, which has been chosen in order to obtain an accurate solution even if the aspect ratio is rather small (e.g. the ratio between the smaller and the larger edges of an element).

In Fig. 5, the quantity of interest considered is the bottom displacement q at the center of the plate in function of the liquid height. At $l = 250$ mm, the absolute value of the displacement is almost 11 times

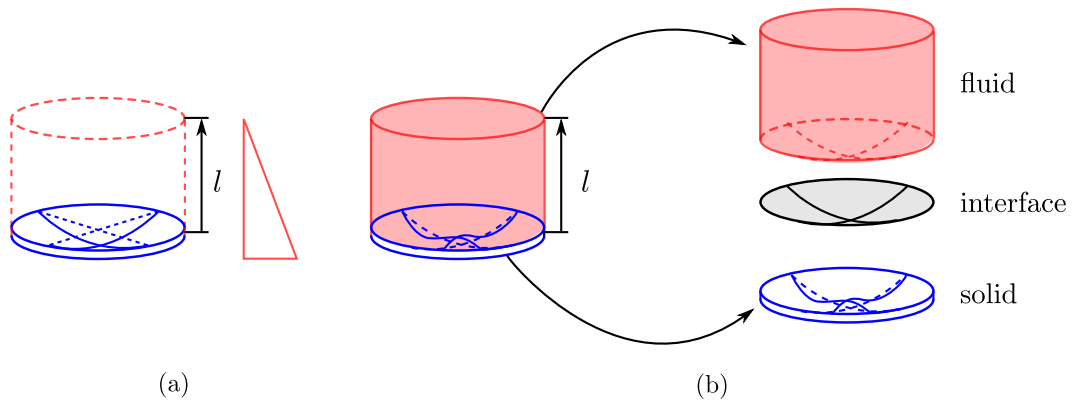

Figure 3: (a) Computation of the prestressed state of the circular plate due to the liquid weight for various liquid height l_i and (b) liquid and structure domains of the linearized hydroelastic vibrations of the prestressed plate.

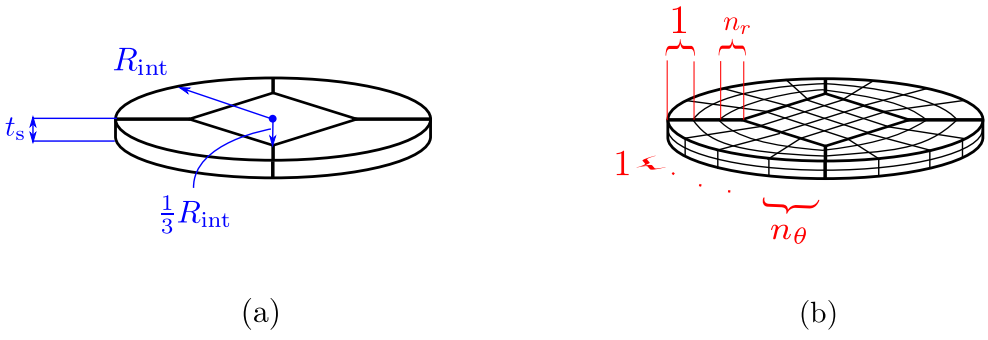

Figure 4: (a) Parameterized geometry with the thickness $t = 0.35$ mm, the internal radius $R_{\text{int}} = 144$ mm; (b) Parameterized mesh by the numbers n_θ and n_{r}, the number of elements in the thickness is fixed as two elements.

higher than the thickness of the structure. Considering this order of magnitude the static solution can be considered in a nonlinear regime. An "overkill" solution denoted by q_{ref}, for a liquid height $l = 250$ mm, has been computed considering a large number of degrees of freedom. Then, simulations have been performed to
225 compare the value of q to the reference as function of the number of elements showing from which the static solution can be considered as independent of the mesh. The table 1 contains all mesh parameters described in Fig. 4.

(n_θ, n_{r})	$(2,2)$	$(5,5)$	$(10,10)$	$(20,20)$	$(50,50)$
n_{elem}	40	250	1000	4000	25000
n_{dof}	771	4380	16995	66965	264009
$q(l = 0.250\,\text{mm})$	-3.12 mm	-3.74 mm	-3.84 mm	-3.86 mm	$q_{\text{ref}} = -3.87$ mm
$100\times \mid q - q_{\text{ref}} \mid / q_{\text{ref}}$	19.3 %	3.4 %	0.77 %	0.25 %	–

Table 1: Results and mesh parametrization.

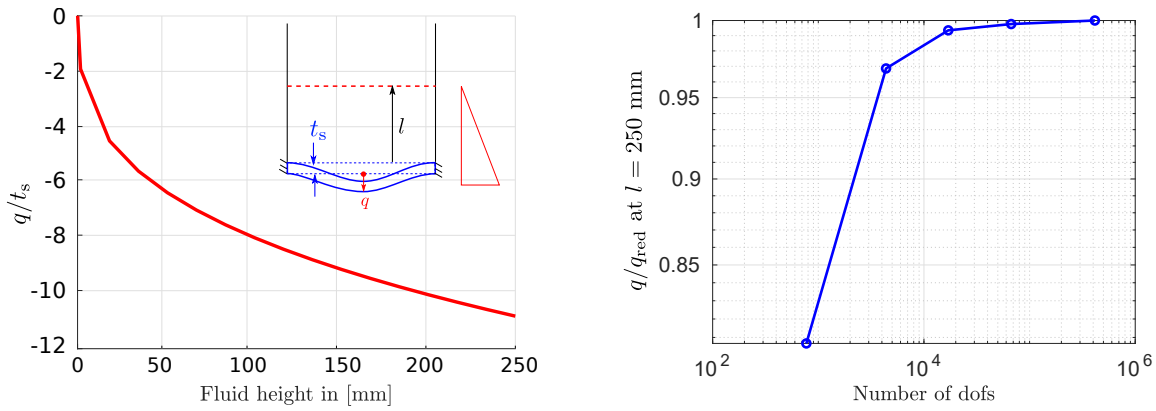

Figure 5: (Left) Evolution of the deflection bottom function of the liquid height with a thickness $t_s = 0.35$ mm and (Right) convergence analysis of the quantity of interest at $l = 250$ mm in function of the number of structural degrees of freedom.

In [18], the deflection value is not measured nor given explicitly given. At this point of the paper, it is not possible to known if the results from the computation are in good agreement with the experiment. Those considerations will be presented later by considering the natural coupled frequencies function of the liquid height. In order to conclude about the static computation, at each liquid height, the nodal static displacement solutions $\mathbf{u}_s^{(i)}$ are known. Thus, the geometrical stiffness matrices $\mathbf{K}_g^{(i)}$, the material stiffness matrices $\mathbf{K}_m^{(i)}$ and the coupling matrices $\mathbf{C}^{(i)}$ needed for the hydroelastic problem can be constructed and stored at those liquid heights. In the sing, we show how to compute the operators $\mathbf{H}^{(i)}$ from a liquid mesh coincident with the solid mesh at the liquid-structure interface.

5.3. Prestressed hydroelastic vibrations

The computation of the hydroelastic natural frequencies needs to mesh the liquid at equilibrium for each liquid height. Here, an associated fluid mesh coincident with the current configuration of the structure is generated as follows. At first, the Fig. 6 illustrates the liquid mesh parameterization that we use to generate a liquid mesh with an appropriate liquid height. Then, the given liquid mesh is deformed using a vector Laplacian equation with a prescribed boundary condition at the liquid structure interface. The risk of distortion is really low because the liquid mesh deformation near the liquid-structure interface is negligible.

Considering the liquid mesh domain, the operators $\mathbf{H}^{(i)}$ are generated for each liquid height l_i. The next step consists in expressing and solving the hydroelastic problem by using the computation methodology presented in Section 4. Considering the geometry of the circular plate, the modal shapes can be characterized by given a couple number (n, m) and a symbol presented in Fig. 7. The number n corresponds to the number of radial waves and m to the angular waves. Those characterizations can still be used for the modal shape of the structural part of hydroelastic modes. In Fig. 8, the hydroelastic natural frequencies are given as function of the liquid height in a frequency range between 0 Hz and 80 Hz. Qualitatively, the graph shows a decrease and then an increase of the natural hydroelastic frequencies for all the modes, except for the first one $(0, 1)$

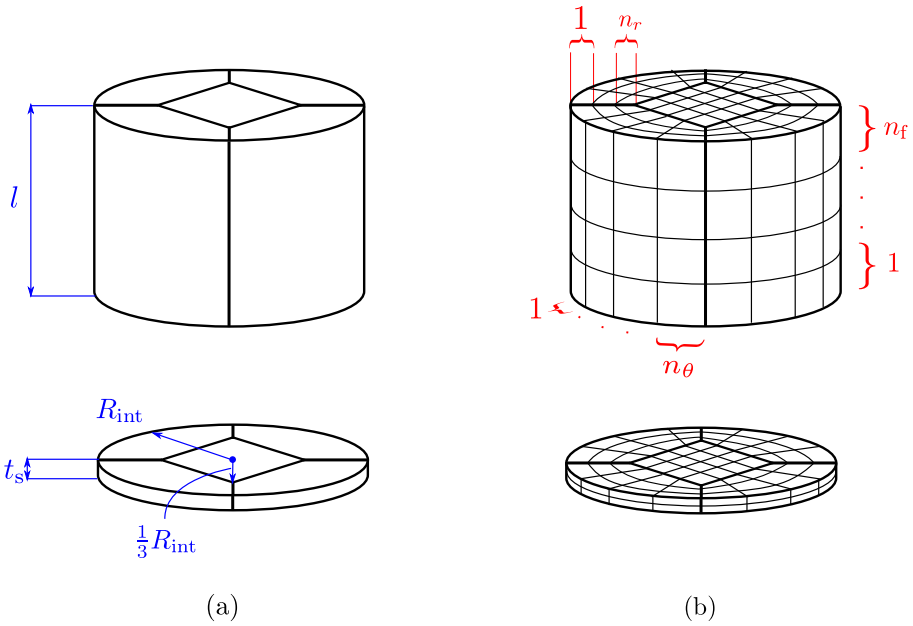

Figure 6: (a) Parameterized geometry of the fluid and the solid of thickness t_{s}, the internal radius R_{int} and the fluid height l; (b) Parameterized mesh with the numbers n_θ and n_{r}.

which have an opposite behavior. The curves are in agreement with the experimental observations presented in reference [18]. We can see that the natural frequencies of the prestressed dry modes tend to increase the natural frequencies in function of the liquid height. Conversely, for an elevation of the liquid height, it is well known that the added mass effect tends to lower the natural hydroelastic frequencies. Therefore, in this example, we have a balance between the prestressed state due to the weight of the liquid and the added mass effect.

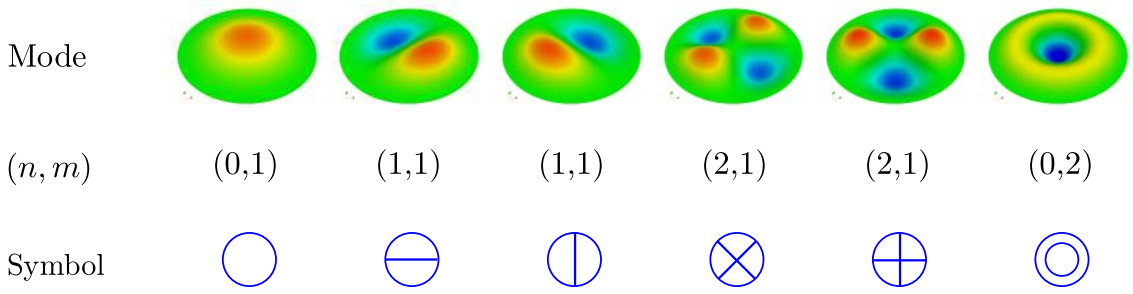

Figure 7: Characterization of the six first modal deformed shapes of the elastic bottom.

At first, for an almost empty structure, a decrease of the natural frequencies can be observed, except for the first mode. At a given height, the natural frequencies reach a minimum value before rising again due to the prestressed effect. In Fig. 9, sectional views of the non-dimensional displacement potential fields are represented respectively for the first and second modes. For the second mode, the spatial fluctuation of potential remains localized near the liquid-structure wall. On contrary, the spatial fluctuation of fluid response for the first mode seems to affect the overall fluid domain. Those observations are in agreement

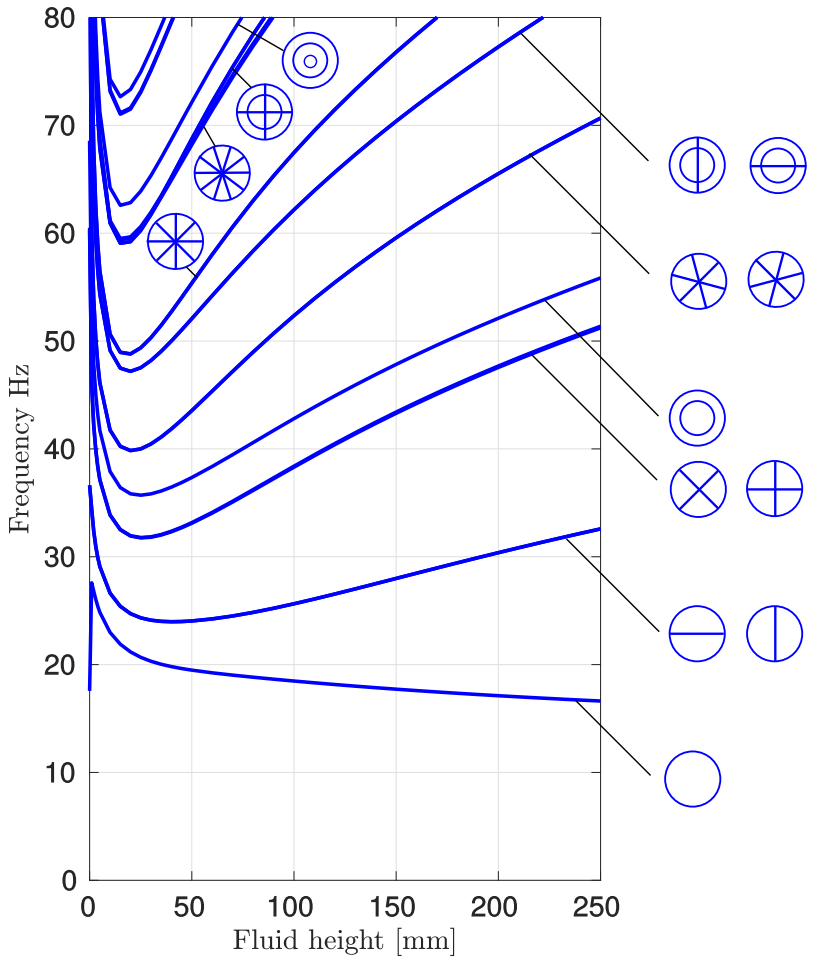

Figure 8: Evolution of the computed hydroelastic natural frequencies as function of the liquid height.

with the behaviour of the evolution of hydroelastic natural frequencies.

The Fig. 10 shows a quantitative comparison between the experiments and the computed natural frequencies which are in very good agreements. When the liquid height l is near zero, differences can be observed. Many uncontrolled parameters can be the sources of those differences : (i) the prestressed effect due to the plate weight without the liquid could be significant at this stage, (ii) the presence of uncertainties of material parameters used in the simulation or (iii) the sloshing effect at the free-surface. Nevertheless, once the liquid height is elevated, a very good agreement between the simulations and the experiments are observed for the first and the third modes. Concerning the second mode, the behavior is overall the same even if a small discrepancy is observed. Numerical results for three particular hydroelastic frequencies are given for various liquid heights in Table 2. A sharp evolution of frequency between an empty state ($l = 0$ mm) and a nearly empty state ($l = 1$ mm) can be observed for the first mode. This behavior is due to the prestress effect as

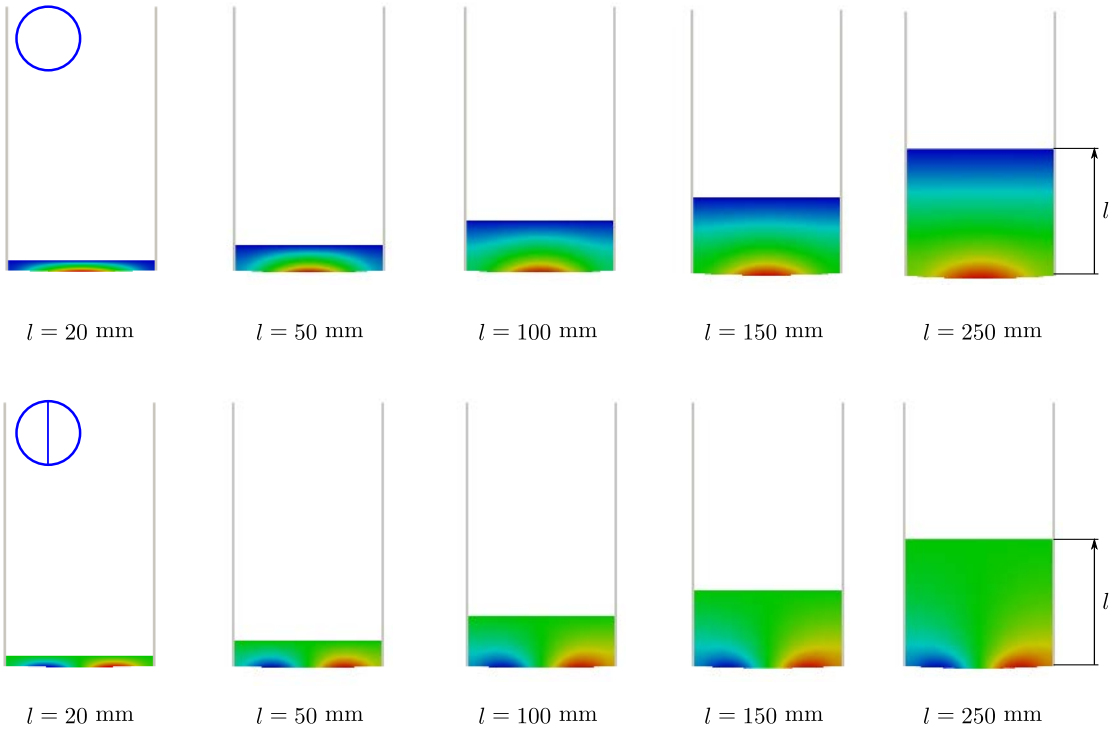

Figure 9: Sectional views of the non-dimensional displacement potential responses for two first modes at various liquid heights.

described in [10].

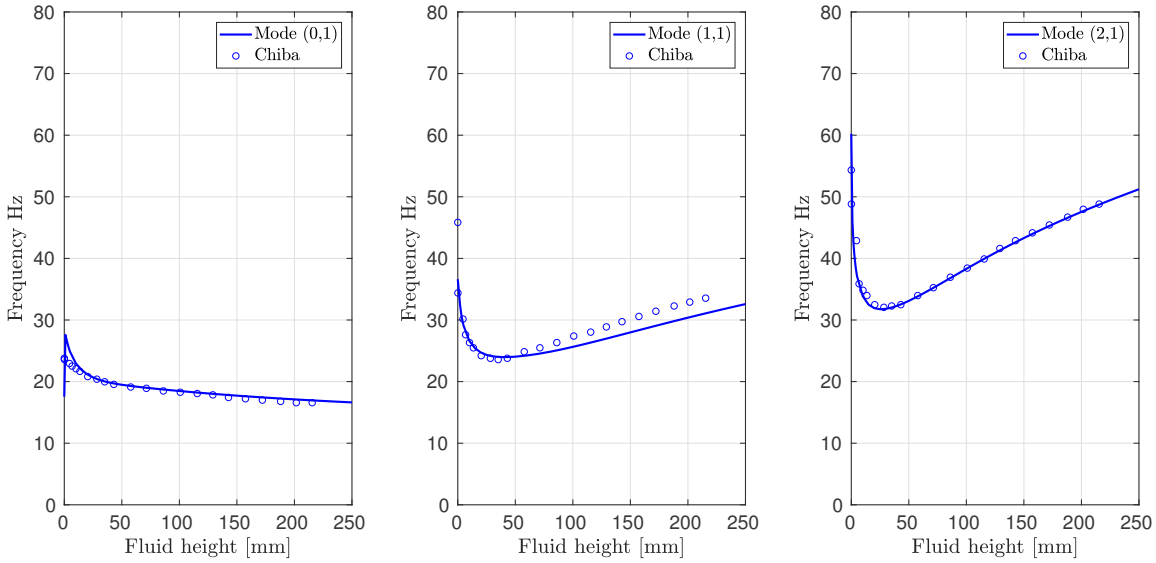

Figure 10: Hydroelastic frequencies as function of the fluid height compared to experimental values extracted from [18].

(n,m)	$l=0$ mm	$l=1$mm	$l=25$ mm	$l=50$ mm	$l=100$ mm	$l=150$ mm	$l=250$ mm
$(0,1)$	17.5 Hz	27.6 Hz	20.7 Hz	19.4 Hz	18.5 Hz	17.8 Hz	16.6 Hz
$(1,1)$	36.6 Hz	34.4 Hz	24.3 Hz	24.0 Hz	25.6 Hz	28.0 Hz	32.6 Hz
$(2,1)$	60.2 Hz	46.0 Hz	31.7 Hz	33.1 Hz	38.3 Hz	43.3 Hz	51.2 Hz

Table 2: Evolution of hydroelastic frequencies (n,m) with prestress effect from liquid weight for various liquid heights.

6. Conclusion

In this paper, we have proposed a numerical strategy for the evaluation of hydroelastic vibrations of an elastic tank containing a free surface liquid, around nonlinear prestressed equilibrium configurations due to the liquid weight. The main originality of the approach lies in the resolution of the problem by considering the liquid height as an evolution parameter. The methodology has been validated by comparison of the numerical solutions with experimental results from the literature. The computation uses the prestressed dry modes on a reference configuration. The numerical methodology presented in this paper is valid for compatible fluid-structure interface meshes. The extension of the methodology for incompatible meshes will be the purpose of future investigations. This would allow more complex parametric situations (e.g. influence of ring stiffeners geometry for example). Deeper convergence analyses are under investigations through appropriate hydroelastic projection-based reduced order models for arbitrary complex 3D shapes.

References

[1] L.-Q. Chen, X. Li, Z.-Q., Lu, Y.-W. Zhang, H. Ding, Dynamic effects of weights on vibration reduction by a nonlinear energy sink moving vertically, Journal of Sound and Vibration 451 (2019) 99–119.

[2] H. J.-P. Morand, R. Ohayon, Fluid structure interaction (1995).

[3] E. H. van Brummelen, Added Mass Effects of Compressible and Incompressible Flows in Fluid-Structure Interaction, Journal of Applied Mechanics 76 (2) (2009) 021206.

[4] R. Ohayon, C. Soize, Q. Akkaoui, E. Capiez-Lernout, Novel formulation for the effects of sloshing with capillarity on elastic structures in linear dynamics, International Journal for Numerical Methods in Engineering 122 (19) (2021) 5313–5330.

[5] H. J.-P. Morand, R. Ohayon, Internal pressure effects on the vibration of partially filled elastic tanks, in: (World Congress on Finite Element Methods in Structural Mechanics, Bournemouth, Hants., England, Oct. 12-17, 1975.) ONERA, TP, no. 1975-66, 1975.

[6] J.-S. Schotté, R. Ohayon, Linearized formulation for fluid–structure interaction: Application to the linear dynamic response of a pressurized elastic structure containing a fluid with a free surface, Journal of Sound and Vibration 332 (10) (2013) 2396–2414.

[7] Y. Bazilevs, K. Takizawa, T. E. Tezduyar, Computational Fluid-Structure Interaction: Methods and Applications, Wiley, 2013.

[8] M. Amabili, Nonlinear Vibrations and Stability of Shells and Plates, Cambridge University Press, 2008.

[9] P. Di Trolio, A. Boldini, M. Porfiri, Modeling added mass effects on the vibrations of air-backed, pre-deformed membranes, Journal of Sound and Vibration 505 (2021) 116149.

[10] M. Chiba, Nonlinear hydroelastic vibration of a cylindrical tank with an elastic bottom, containing liquid. part II: Linear axisymmetric vibration analysis, Journal of Fluids and Structures 7 (1) (1993) 57–73.

[11] A. W. Leissa, Vibration of Shells, Vol. 288, Scientific and Technical Information Office, National Aeronautics and Space, 1973.

[12] M. Amabili, M. P. Païdoussis, Review of studies on geometrically nonlinear vibrations and dynamics of circular cylindrical shells and panels, with and without fluid-structure interaction, Appl. Mech. Rev. 56 (4) (2003) 349–381.

[13] M. Amabili, I. D. Breslavsky, Displacement dependent pressure load for finite deflection of doubly-curved thick shells and plates, International Journal of Non-Linear Mechanics 77 (2015) 265–273.

[14] M. Haßler, K. Schweizerhof, On the static interaction of fluid and gas loaded multi-chamber systems in large deformation finite element analysis, Computer Methods in Applied Mechanics and Engineering 197 (19-20) (2008) 1725–1749.

[15] C. Hoareau, J.-F. Deü, Nonlinear equilibrium of partially liquid-filled tanks: A finite element/level-set method to handle hydrostatic follower forces, International Journal of Non-Linear Mechanics 113 (2019) 112–127.

[16] N. Narayanan, R. Wuechner, J. Degroote, Monolithic and partitioned approaches to determine static deformation of membrane structures due to ponding, Computers & Structures 244 (2021) 106419.

[17] B. E. Griffith, N. A. Patankar, Immersed methods for fluid–structure interaction, Annual review of fluid mechanics 52 (2020) 421–448.

[18] M. Chiba, Nonlinear hydroelastic vibration of a cylindrical tank with an elastic bottom, containing liquid. part I: Experiment, Journal of Fluids and Structures 6 (2) (1992) 181–206.

[19] P. G. Ciarlet, Mathematical Elasticity: Volume I: three-dimensional elasticity, North-Holland, 1988.

[20] K.-J. Bathe, Finite Element Procedures, Klaus-Jurgen Bathe, Watertown, MA, 2006.

[21] P. Wriggers, Nonlinear Finite Element Methods, Springer, 2008.

[22] R. De Borst, M. A. Crisfield, J. J. Remmers, C. V. Verhoosel, Nonlinear Finite Element Analysis of Solids and Structures, Wiley, 2012.

[23] T. Belytschko, W. K. Liu, B. Moran, K. Elkhodary, Nonlinear Finite Elements for Continua and Structures, Wiley, 2014.

[24] H. Hibbit, Some follower forces and load stiffness, International Journal for Numerical Methods in Engineering 14 (6) (1979) 937–941.

[25] I. Elishakoff, Controversy associated with the so-called "follower forces": critical overview, Appl. Mech. Rev. 58 (2) (2005) 117–142.